

Dynamic response and deformation characteristics of urban loess subgrade under vehicle load

Liu Yipin

China Railway 19 Bureau Group Rail Transit Engineering Co., Ltd 813399

Received 13 September 2022

Abstract

Urban road disasters in the northwest loess area are frequent. Owing to the cracking and dislocation of the road surface caused by the quality of the subgrade engineering and the circulating load of the vehicle, the settlement and deformation of the subgrade are prominent. These issues pose hazards to the normal operation of urban roads and the safety of residents. On this basis, this paper uses Abaqus numerical analysis software to establish a 3D solid model of the actual road structure system. The indoor shear strength of the actual roadbed soil is tested, and the dynamic response law and settlement deformation characteristics of the loess subgrade under different moisture content, dry density, and vehicle load conditions are examined. This study strives to provide a reference for disaster prevention and mitigation of urban roads in the northwest loess region. Results show that under the action of vehicle load, the vertical strain and vertical displacement of the loess subgrade have an attenuation trend from shallow to deep. The attenuation rate shows a shallow, fast, deep, and slow change mode. The influence depth of standard vehicle-15 grade wheel load is about 4.5 m under the road surface, and plastic deformation diffusion occurs along the depth of the roadbed. The cumulative settlement deformation of the subgrade loess shows a gradual growth trend with the accumulation of cyclic vibration, demonstrating the phenomenon of large deformation in the early stage and stable development in the later stage. The loess structure of the subgrade will become more dense and the strength will be improved after multiple cycle vibrations. Under the action of vehicle load, the sedimentation deformation of loess subgrade increases with the growth of moisture content and load, and decreases with the growth of dry density. Thus, water control and load control can effectively control the rate of road disasters such as loess subgrade deformation and settlement.

© 2023 The Institution of Engineers, Bangladesh. All rights reserved.

Keywords: Loess subgrade, vehicle loads, numerical simulation, dynamic response, morph features.

1. Introduction

With the steady advancement of China's "Western Development Strategy," urbanization in the loess region of Northwest China has rapidly developed. Along with the construction and widening of urban roads, the number of urban traffic vehicles is increasing day by day. Hence, the impact of vehicle load on the road structure has become evident (Lin, M.A., et al.,

2018; Daxin, G., et al., 2021; Gouchen, Z., et al., 2020; Qi, H., et al., 2022), and the safety problems arising from such has become a major concern in society. In recent years, urban road disasters have occurred frequently. Cracking and misalignment of post-work pavement caused by the load of traffic vehicles, and disasters such as subgrade settlement and deformation are particularly prominent. Moreover, they pose hazards to the normal operation of urban roads and the safety of residents. According to the relevant investigation and analysis, the occurrence of this phenomenon has an important correlation with the soil engineering properties of road subgrades, the vibration effect of vehicle load on the road surface, and other factors (Bin, Y., et al., 2012; Luo, J., et al., 2019; Rui, W., et al., 2021; Gang, S., et al., 2020). Thus, the dynamic response and deformation characteristics of urban loess subgrades under vehicle load have become the focus of social concern.

Settlement deformation of the road subgrade is common, and it results in the dislocation and cracking of pavement structure. Many scholars have done substantial research in this regard, and the results have a certain guiding effect on the actual project. Foreign scholars intervened in the study of subgrade deformation earlier. They defined vehicle load form as a dynamic load model, believing that the semi-sine wave and the sine wave are more in line with the transmission form of vibration wave in the vehicle and road subgrade system (O'connor A. and O'brien E. J., 2005). Scholars (Ishikawa T. and Miura S. 2015) used the single-stage loading method and the moving wheel loading method to conduct dynamic tests on the subgrade fill materials under saturated and unsaturated states. They studied the applicability of the torsional shear test to the simulated vehicle load on the roadbed soil, as well as the influence of moisture content and moving vehicle load on the deformation characteristics and strength characteristics of the roadbed soil. The results showed that the synergistic effect of the rotation of the principal stress axis and the change of moisture content on the plastic deformation of the roadbed soil must be considered. Scholars (Thevakumar, K., et al., 2021) consider the long-term mechanical behavior of the roadbed soil, explore the way of imposing a long-term cyclic overload, conduct experimental tests with different cumulative cycle stress sizes and cycle cycles as parameter variables, compare and analyze the similarities and differences of the test results, and finally determine the relevant parameters affecting the roadbed soil. Similar research by foreign scholars presents rich results, and most of them are aimed at guiding practical engineering; hence, their specific environments and conditions have an impact on the deformation of roadbed soil (Hwang, S. K., 2004; Ishikawa, T., et al., 2008; Ashpiz, E. S. and Zamukhovskiy, A. V., 2017).

Domestic research in the sedimentation deformation of roadbed soil is even more fruitful, and the research results have great guiding significance for the actual engineering environment in China. On the basis of field experiments, Yang Qiangqiang et al., 2021 studied the transmission and diffusion law of vertical pressure of loess subgrade under vehicle load by measuring the vertical earth pressure at different speeds and different loads in different depth subgrades. Through the dynamic monitoring of the soil pressure of the road subgrade under the action of fill soil and vehicle load vibration, Wang Xinzhi et al., 2018 systematically studied the transmission and distribution characteristics of pressure in calcareous sand subgrade soil. Their findings provided a practical basis for the application of similar new materials. Meng Shangjiu et al., 2018 used optical fiber Bragg grating technology to monitor the development status of dynamic deformation of subgrade, combined with on-site monitoring data, through FLAC3D simulation software to simulate the dynamic deformation of subgrade under vehicle load, efficient and reasonable analysis of subgrade dynamic deformation response, providing technical means for road engineering construction. Moreover, owing to the maturity and intervention of numerical simulation, the problem of subgrade deformation under vehicle load has been further deepened (Huan, Y., et al., 2017; Jun, Z., et al., 2014; Zhongming, H., et al., 2020). It provides effective numerical analysis and

optimization for complex and diverse practical projects, and provides convenience and guarantee for the construction of urban roads. In summary, the collective research on the deformation of the subgrade under vehicle load has achieved results. However, only a few studies have been conducted on the urban loess subgrade, which needs to be explored. Hence, this paper considers the stratification of various structures of the pavement, establishes a 3D road model, and studies the dynamic response law and settlement deformation characteristics of the loess roadbed under the action of vehicle load through finite element analysis method. The research results can provide relevant reference for disaster prevention and mitigation of urban roads.

2. Numerical modeling

2.1 Road model

In this paper, ABAQUS simulation software is used to analyze numerically the dynamic response and settlement deformation of urban loess subgrade under traffic load. Figure 1 shows the 3D road structure system. Using the symmetrical system of the actual urban road structure as a model, the overall length of the model is 20 m, the width is 80 m, the height is 6 m, and it is along the X axis. In order to make the calculation efficient and obtain accurate calculation results, the mesh division of the shallow position at the vehicle's two wheels is dense, and the mesh transitions from dense to sparse as the depth of the model increases.

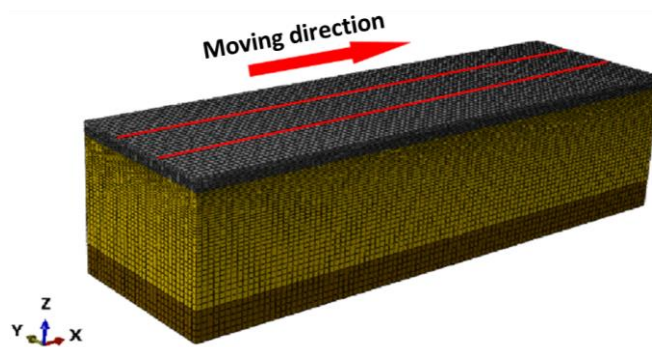


Fig. 1. Geometric model of a 3D road structure.

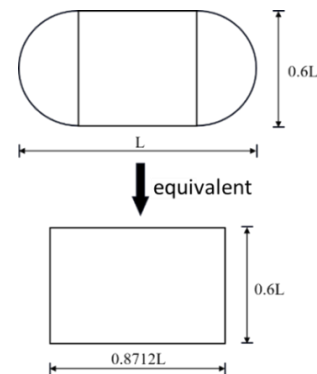


Fig. 2. Conversion of tire contact area.

The road structure layer is divided into four parts: the pavement layer (0.15 m), the base layer (0.55 m), the loess roadbed (4.30 m), and the ground base (1.00 m). The actual road surface layer is mostly asphalt concrete material and the base layer is mostly rigid or semi-rigid gravel concrete material, so the surface layer and the base layer are defined by elastic constitutive model. Moreover, the loess roadbed and the ground base are defined by elastoplastic constitutive model. Table 1.1 shows the material parameters of each layer.

Table 1.1
Model material parameters

Material type	density / $\text{kg}\cdot\text{m}^{-3}$	modulus / MPa	Poisson's ratio
Surface course	2,500	1,500	0.25
basic level	2,200	1,200	0.25
Loess subgrade	form 1.2	60–100	0.35
Foundation strata	40	0.35	1930
Material type	Cohesion / kPa	Internal friction angle / $^{\circ}$	Damping ratio
surface course	—	—	0.15
basic level	—	—	0.15
Loess subgrade	form 1.2	form 1.2	0.08
Foundation strata	45	28	0.15

Among them, for the relevant soil conditions of loess subgrade, the direct shear test is carried out on the preparation of different moisture content and dry density of loess of a certain subgrade in Shaanxi, and the ZJ type strain-controlled straight shear instrument is used. The trial data were calculated using the Mohr–Coulomb criterion, which is as follows:

$$\tau = c + \sigma \tan \varphi \quad (1.1)$$

where τ is the shear stress; σ is the total stress; and c is the cohesion of the soil. φ is the internal friction angle of the soil. Table 1.2 shows the shear strength index of loess under different moisture content and dry density. After the basic model is established and considering the damping characteristics of each layer, the damping coefficient of the model is set. The Rayleigh linear damping is used to define, Abaqus software is used to conduct modal analysis of each structure, and the first- and third-order self-resonant circular frequencies are selected for the calculation of damping parameters. Considering that the vehicle load waveform touches the model boundary during the transmission process, it will reflect the effect, so the model boundary is set by a 3D viscoelastic artificial boundary.

Table 1.2
Shear strength index of specimens

Moisture content (%)	Dry density (g/cm ³)	density (g/cm ³)	Cohesion (kPa)	internal friction angle (°)
14%	1.25	1.43	23.6	21.6
	1.45	1.65	30.4	24.8
	1.65	1.88	39.3	27.2
18%	1.25	1.48	20.8	20.1
	1.45	1.71	27.9	22.5
	1.65	1.95	34.6	24.7
22%	1.25	1.53	15.5	18.9
	1.45	1.77	18.2	20.7
	1.65	2.01	22.8	22.3

2.2 Loading form of vehicle load

This paper uses the VDLOAD subroutine embedded in the Abaqus software for load definition and application. The standard vehicle type of Automobile -15 class was selected as the reference basis for vehicle load. The standard axle load of the rear wheel was 100 kN; the wheelbase between the rear wheels of the vehicle was 2 m; the single-wheel axle load was 25 kN; and the tire pressure was 700 kPa. On the basis of this standard, 300 kPa and 500 kPa were taken as the control variable groups for calculation and analysis. In the process of road driving, the vehicle is regarded as a vibration system of the double degree of freedom simplified model, and the whole is superimposed by the vehicle's own weight and vibration dynamic charge. Its action form can be expressed as:

$$P = P_s + P_d \quad (1.2)$$

In the formula, P_s is the static load size of the vehicle; P_d is the dynamic load amplitude of the vehicle when it is running, where the dynamic load coefficient is taken, and the value of this simulation is 0.12; ω is the vibration circular frequency, that is, the size of the vehicle is affected by the driving type and driving speed; v is the driving speed; L is the length of the vehicle geometry curve, 4 to 6 m. For the form of contact between the wheel and the road surface, the ellipse contact is usually approximately equivalent to a rectangular contact according to the principle of area equivalence, as shown in Figure 2. Equation 1.3 shows the conversion formula.

$$L = \sqrt{F/0.5227p} \quad (1.3)$$

where F is the standard axle load (kN) for a single wheel and p is the tire pressure (kPa) of a single wheel.

2.3 Basic assumptions

In order to make the finite element model realistic during the analysis process and to facilitate the analysis and calculation, basic assumptions about the model must be established:

1. The surface layer and the base layer under the action of vehicle load are elastic models, and the materials of the loess subgrade and the ground base are uniform and conform to the elastoplastic small deformation model;
2. The displacement between the layers is completely continuous, and the sliding contact between the adjacent layers is not considered;
3. During the vibration loading process, the material parameters of the structure are not changed;
4. The initial stress of loess is mainly the self-gravity stress and lateral earth pressure of the soil.

3. Dynamic response analysis of loess subgrade

3.1 Strain change law

Under the action of vehicle load, the loess subgrade under the wheel shows the greatest vertical strain at the top layer. With the increase of depth, the strain decays during the transmission process and finally gradually balances at the bottom of the subgrade. Figure 3 shows the vertical strain curves at different depths ($w=18\%$, $\rho_d=1.45 \text{ g/cm}^3$, $P_s=700 \text{ kPa}$).

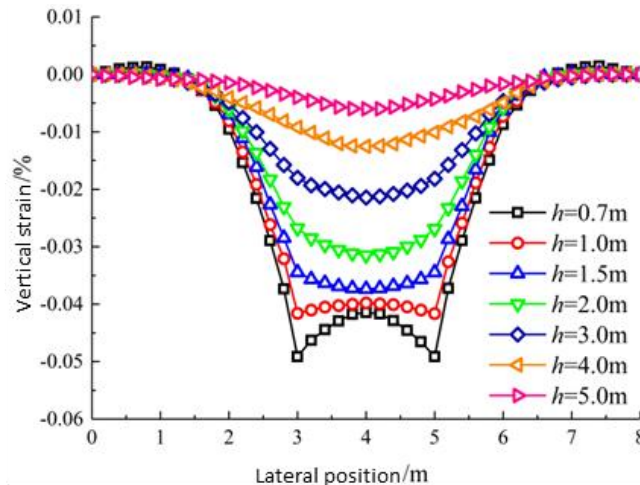


Fig. 3. Variation law of vertical strain of loess subgrade.

At 0.7 m at the top layer of the loess roadbed directly below the wheel, the plastic strain of the soil body is the largest, and the horizontal strain shows a near-fast and long-range decay trend. At the top layer of the subgrade 2 m from the wheel, the soil appears in a small tensile strain state. The tensile strain only exists in the shallow position of the subgrade soil, and the tensile strain will gradually disappear with the increase of depth. The strain attenuation of the subgrade soil gradually decreases with the increase of depth, and the shape of the strain curve at the deep layer also changes from peak-tip to parabolic.

In soil dynamics, the variable level of 0.01% is used as the boundary between large strain and small strain, so 0.01% is used as the criterion for the influence depth of vertical dynamic strain. As shown in Figure 3, the maximum influence depth of the strain at $P_s=700$ kPa is about 4.5 m.

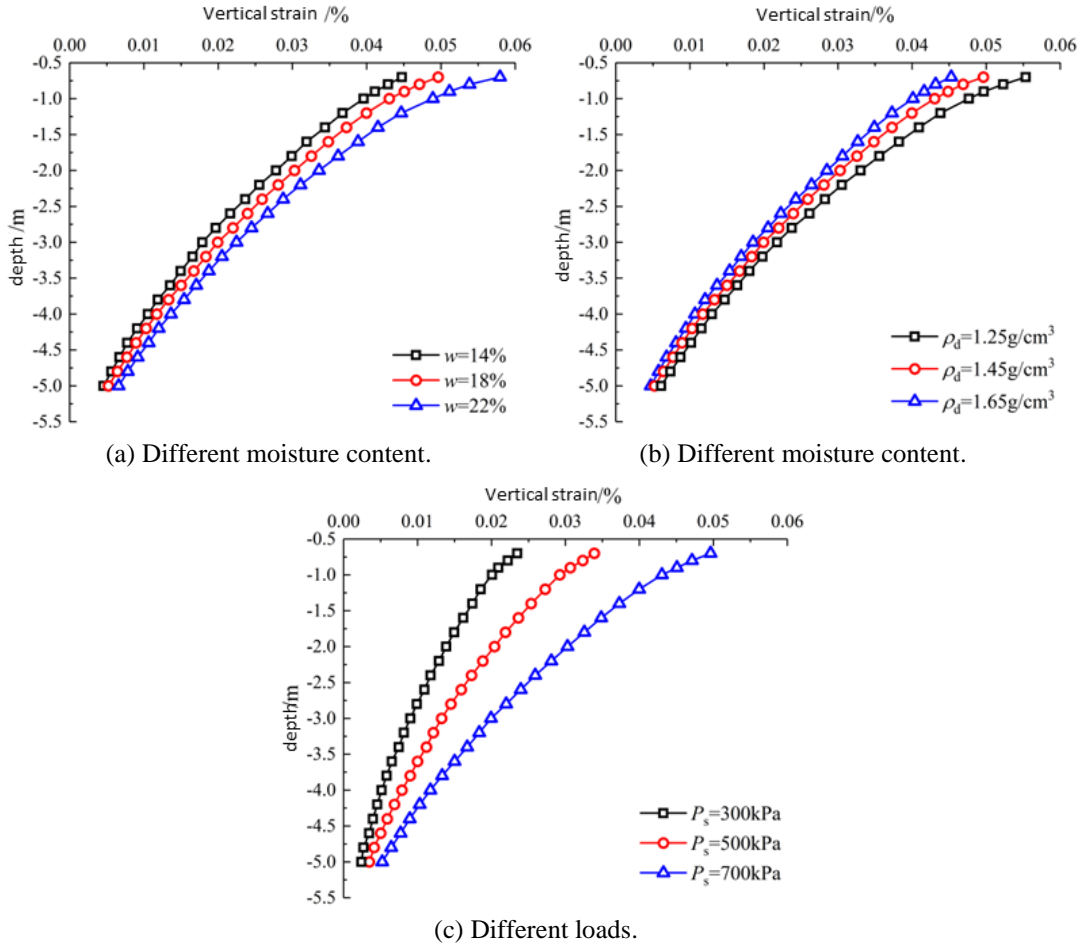


Fig. 4. Vertical strain–depth curve of loess subgrade under wheel.

As shown in Figure 4, under the action of vehicle load, the vertical strain of the loess subgrade gradually decreases with the increase of depth. The attenuation rate of the strain at the shallow layer is fast, and the vertical strain drops to 0–0.01% at the bottom 5 m. Under different moisture content, its vertical strain increases with the increase of moisture content. The increase in the shallow layer of the soil is relatively significant: the moisture content increases from 14% to 22%, the vertical strain increases from 0.044% to 0.058%, and the strain difference at the bottom layer is small. The increase of moisture content thickens the water film between soil particles, resulting in a decrease in the mutual staggering resistance of particles.

Additionally, the vertical strain caused by high moisture content under the same vibration force is increased, and the degree of deformation becomes evident. The vertical strain of the loess subgrade increases with the increase of dry density, and the larger dry density inhibits the plastic strain of the subgrade soil. When the dry density is increased from 1.25 g/cm^3 to 1.65 g/cm^3 , the top layer strain is reduced from 0.056% to 0.045%. The amplitude of the vertical strain of the shallow subgrade is large, and the amplitude of the strain gradually decreases with the increase of depth. The increase of dry density intuitively reflects the

increase of soil particles per unit volume, the increase of contact area between particles, the increase of soil resistance to vibration deformation, and the improvement of soil stiffness and strength.

The impact of vehicle load size on the vertical strain of the loess subgrade is the most obvious. When the load is reduced from 700 kPa to 300 kPa, the vertical strain of the top layer of the soil is reduced from 0.049% to 0.024%, and the amplitude is greater than the moisture content and dry density. As a dynamic condition, the influence of the size of the vehicle load on the roadbed soil is concentrated in the shallow soil area under the wheel. The plastic strain range circle inside the soil is characterized by enlargement, and the overall strain attenuation with the road and depth is significant.

3.2 Law of displacement change

The vertical displacement of the loess subgrade section with the depth under the action of vehicle load is more significant, and the degree of depression and deformation magnitude of the subgrade soil at different depths are also more intuitive, as shown in Figure 5.

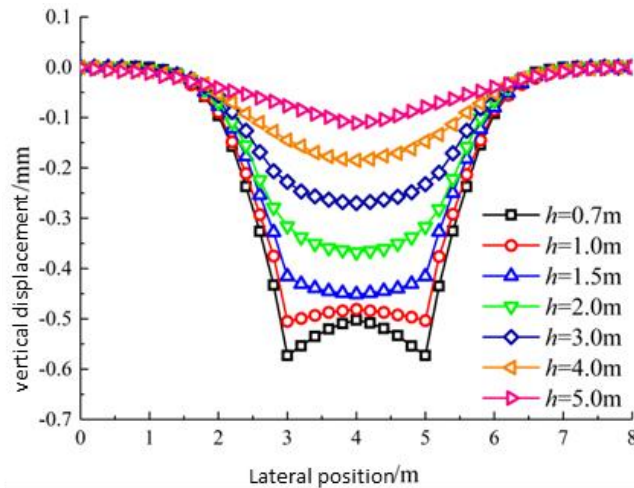


Fig. 5. Variation of vertical displacement of loess subgrade.

The top of the loess roadbed at 0.7 m below the wheel produces the largest amount of displacement deformation, followed by rapid attenuation in the horizontal direction. The vertical displacement at about 2.0 m on both sides of the contact surface is approximately attenuated to 0.0 mm. With the increase of depth, the degree of vertical displacement deformation in the soil is generally manifested as a form of large shallow layer and small depth. The vertical displacement decay of the bottom layer of the soil body is about 81% at the top layer, and the decay rate is from urgent to slow. The vertical displacement deformation at different depths gradually decreases to both sides, showing a decay trend of near, fast, and far. The curve is basically distributed in a central symmetrical form. The overall analysis found that the displacement deformation at a distance of 1.8 m to 3.0 m from the wheel was approximately attenuated to 0.0 mm, and the influence range of plastic deformation was significantly expanded with the increase of depth. Its curve form also transitioned from peak-tip type to parabolic distribution gradient.

The curve change law shown in Figure 6 shows that the vertical displacement of the loess subgrade presents a gradual decay trend with depth under different conditions. The vertical displacement at the shallow layer of the subgrade is faster than that of the deep layer, and the

displacement deformation to the bottom layer of the soil body is in the range of 0.04–0.12 mm. The increase of moisture content on the vertical displacement of loess is very significant: the moisture content of the soil increased from 14% to 22%, the maximum value of the shallow vertical displacement increased from 0.48 mm to 0.72 mm, and the deformation amount increased by about 56.5%. The displacement at the bottom layer increased from 0.09 mm to 0.12 mm, and the amount of deformation increased by about 33.3%. The analysis shows that the shallow loess under the vehicle load is evidently affected by the moisture content, whereas the displacement deformation of the deep soil is small. The increase of moisture content increases the amount of deformation generated by the soil body being loaded. In addition, the original frictional resistance between the loess particles is reduced, the degree of mutual stagger deformation is intensified, and the shallow soil body is more significant. Hence, the actual deformation degree of the subgrade depression is particularly affected by moisture content.

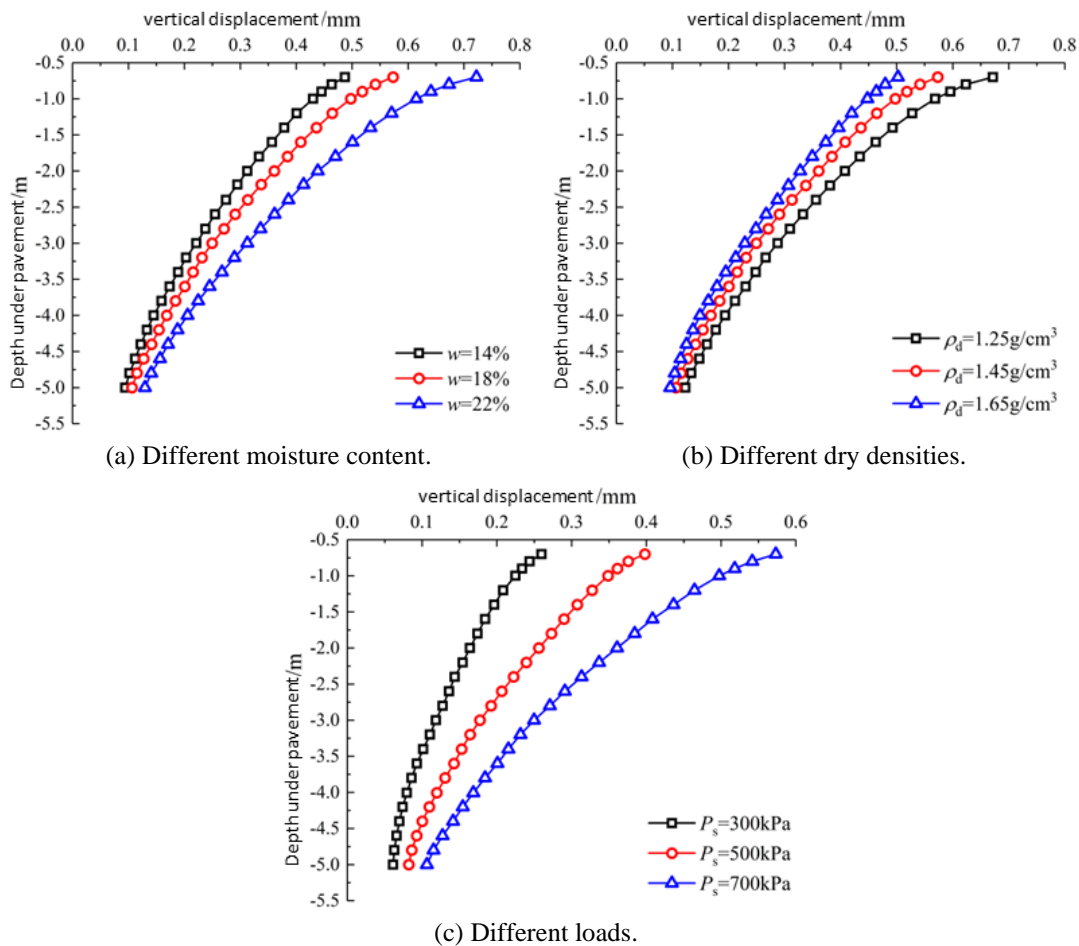


Fig. 6. Vertical strain–depth curve of loess subgrade under wheel.

As shown in Figure 6(b), the vertical displacement of shallow subgrade loess under 1.25 g/cm³ dry density is about 0.67 mm, whereas the maximum displacement deformation of 1.65 g/cm³ dry density is about 0.50 mm. Moreover, the vertical displacement of the soil body gradually decreases with the increase of dry density, and the reduction gradually decreases. The increase of dry density increases the pore filling rate inside the soil, the degree of deformation caused by the mutual staggering of the particles under the influence of vehicle load is weakened, and the friction resistance between the particles increases the ability to resist the vertical displacement deformation of the soil, and the allowable space for

deformation is reduced. As a result, the longitudinal displacement deformation amplitude of the soil is reduced.

The vehicle load is reduced from 700 kPa to 300 kPa, the maximum vertical displacement of the top layer of the shallow roadbed is reduced from 0.58 mm to 0.26 mm, and the deformation is reduced by about 55%. In addition, the maximum vertical displacement of the soil bottom is reduced from 0.11 mm to 0.06 mm, which is greatly reduced from the top layer difference, and the vertical displacement decays rapidly with the increase of depth. The influence of load growth on the loess of the subgrade is large, the displacement deformation attenuation is fast, the plastic deformation range is wide, and the influence on the settlement deformation of the soil is the most intuitive.

4. Analysis of the law of cumulative settlement deformation of loess subgrade

In the actual urban road environment, the long-term effect of vehicle loads causes the loess subgrade to produce deformation characteristics gradually such as settlement and depression. With the continuous action of vehicle circulating vibration, the plastic deformation of the soil under a single vibration accumulates sequentially, showing the gradual increase of the settlement deformation of the loess roadbed. Therefore, the top layer of the loess roadbed directly below the wheel is selected, and the cumulative settlement displacement deformation law of the vehicle load cycle under different working conditions is analyzed (standard working condition $w=18\%$, $\rho_d=1.45 \text{ g/cm}^3$, $P_s=700 \text{ kPa}$), as shown in Figure 7.

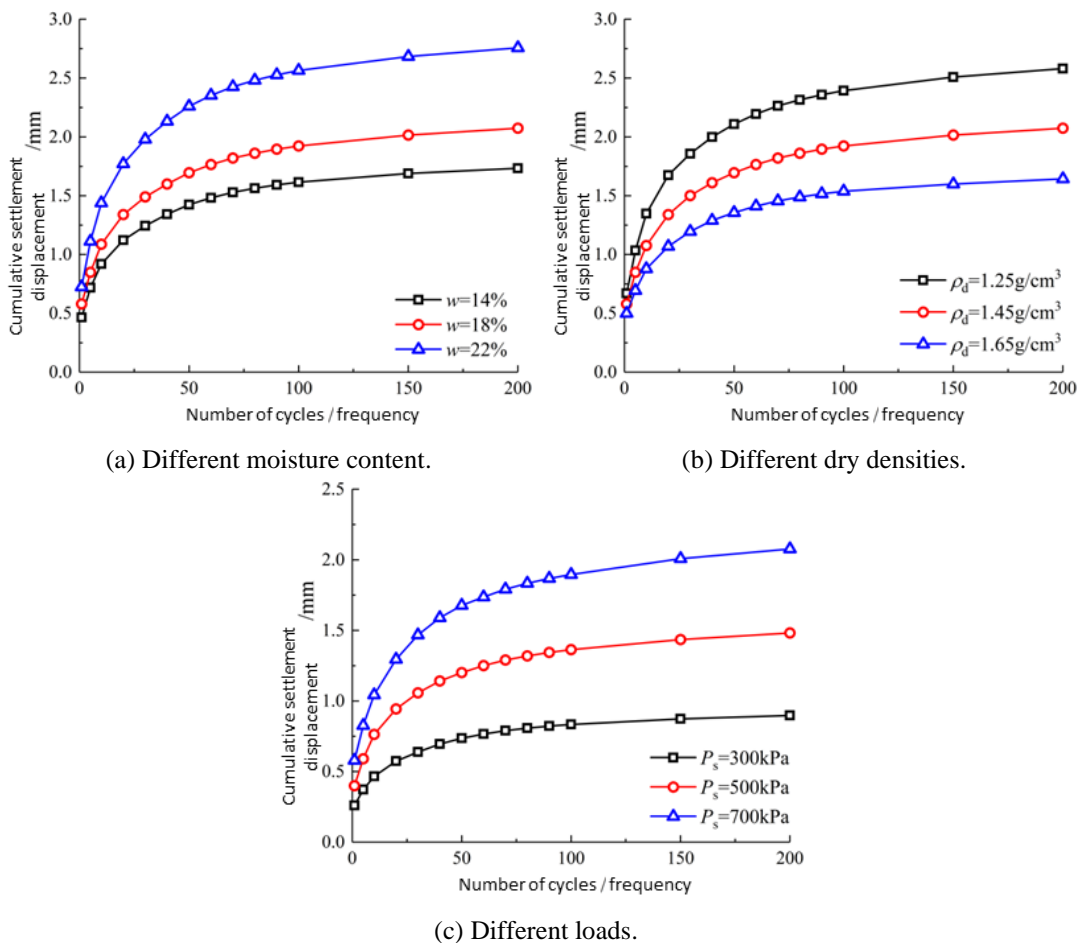


Fig. 7. Relationship curve between cycle times and cumulative settlement displacement of loess subgrade under wheel.

The curve changes in Figure 7 show that the subgrade loess will produce an initial vertical displacement during the initial vibration, and the development of the cumulative settlement displacement gradually increases with the increase of the number of cyclic loadings. However, the growth rate gradually weakens, and the tangent slope of the curve decreases continuously. The cumulative action process was analyzed, and the cumulative sedimentation displacement under the previous 1–20 cycles developed rapidly. The cumulative displacement increase of 20 to 100 cycles gradually decreases. After 100 cycles, the cumulative sedimentation deformation tends to develop steadily, and the increase is small.

Under different moisture content conditions, the vertical displacement of the top layer of the loess roadbed increases with the increase of moisture content, and the increase rate gradually decreases with the cumulative cycle vibration. Compared with the cumulative sedimentation displacement development law of remodeling loess at $w=14\%$ and $w=22\%$ moisture content, the displacement difference between the two is about 0.26 mm when it is vibrated once, about 0.85 mm when it is vibrated 50 times, and about 1.00 mm when it is vibrated 200 times. The growth rate of the cumulative sedimentation displacement is fast within the first 50 vibrations, and then gradually decreases and flattens out. The increase of moisture content reduces the friction between soil particles, aggravates the staggered slip between particles, and increases the displacement deformation of subgrade loess under high moisture content. Moreover, the growth rate gradually increases within a certain moisture content range. The development of cumulative settlement deformation under different dry densities is contrary to the moisture content conditions. When the dry density is 1.25 g/cm^3 , 1.45 g/cm^3 , and 1.65 g/cm^3 , the vertical deformation difference caused by the vehicle load accumulation cycle of 200 times is about 0.53 mm and 0.40 mm. With the increase of dry density, the vertical displacement of the top layer of the roadbed soil is gradually reduced, and the reduction is gradually reduced. The increase of dry density leads to an increase in the number of soil particles per unit volume. Moreover, the contact between particles is relatively close, and the pores in some areas are filled. Hence, the deformation of soil with large dry density is small and shows a nonlinear change trend.

The influence of vehicle load on the cumulative settlement displacement of subgrade loess is the most intuitive, which belongs to the plastic deformation caused by the vibration load of the soil. After 200 cycle vibrations, the cumulative displacement deformation generated by the 300 kPa load is about 0.89 mm, which is 1.48 mm at 500 kPa load and 2.06 mm at 700 kPa load. The strain growth is obviously positively correlated with the load increase. The increase of vehicle load significantly improves the degree of vertical displacement deformation and influence range of the loess of the subgrade. When the vehicle load exceeds a certain limit value, the structural damage of the loess subgrade will be further deepened. In the case of repeated action of the moving load, the speed and degree of settlement deformation of the subgrade soil are accelerated. Hence, strict control of the type and load of traffic vehicles is necessary.

5. Conclusion

In this paper, the dynamic response law and settlement deformation characteristics of loess subgrade under different moisture content, dry density, and vehicle load conditions are examined using Abaqus numerical analysis software and indoor shear test. The main conclusions are as follows:

- In the plane perpendicular to the vehicle load and along the depth direction, the vertical strain and vertical displacement of the loess subgrade have an attenuation trend of transition from a shallow layer to a smaller depth. The attenuation rate shows a shallow,

fast, and deep change mode. For standard vehicles, the depth of influence of the 15-stage wheel load is about 4.5 m below the road surface. At the same time, the vertical strain and vertical displacement curves that change with depth in the horizontal direction are transitioned from peak-tip type to parabolic type, and a phenomenon of plastic deformation diffusion occurs.

- Under the action of vehicle load, the vertical strain and vertical displacement of the loess subgrade increase with the growth of moisture content and load, and decrease with the increase of dry density. Moisture content and dry density are used as soil conditions for subgrade, and the changes of both have mutual restriction effects. As a dynamic condition, vehicle load has a relatively single impact on the deformation of the roadbed. Therefore, in the construction of urban roads in the loess area, water control and load control can effectively control the incidence of road disasters such as deformation and settlement of loess subgrade.
- The cumulative cyclic effect of urban vehicle load has an impact on the settlement deformation of the loess subgrade. The study shows that the cumulative sedimentation deformation of the subgrade loess presents a gradual growth trend with the accumulation of cyclic vibration, and its growth rate is manifested as a phenomenon of large deformation in the early stage and stable development in the later stage. Furthermore, the cumulative settlement deformation of the loess subgrade gradually increases with the increase of moisture content, the decrease of dry density, and the increase of vehicle load. These results show a nonlinear change trend, and the loess structure of the subgrade will become denser after multiple cycle vibrations, and the soil strength will be improved.

References

- Ashpiz E S, Zamukhovskiy A V. Subgrade strengthening on the sections for cars interchanging with axle load of 25 T and more(J). *Procedia engineering*, 2017, 189: 874-879.
- Geng Daxin, Yang Zechen, Wang Ning. Research on the Stress Response of Highway Subgrade Caused by Dynamic Traffic Load(J). *Highway*, 2021, 66(12): 1-7.
- He Zhongming, Qiu Junjun, Ke Wei. Analysis of dynamic characteristics of coarse-grained soil high embankment under traffic load(J). *Journal of Central South University (Science and Technology)*, 2020, 51(09): 2571-2579.
- Hwang SK. Settlement Characteristics of the Reinforced Railroad Roadbed with Crushed Stones Under a Simulated Train Loading(J). *Journal of the Korean Geotechnical Society*, 2004, 20(2): 5-13.
- Ishikawa T, Hosoda M, Miura S, et al. Influence of water content on mechanical behavior of gravel under moving wheel loads(J). *Advances in Transportation Geotechnics*, Ellis, E., Thom, N., Yu, HS, Dawson, A., and McDowell, G.(eds.), 2008: 185-191.
- Ishikawa T, Miura S. Influence of moving wheel loads on mechanical behavior of submerged granular roadbed(J). *Soils and Foundations*, 2015, 55(2): 242-257.
- Luo J, Liu X, Mi D, et al. Intelligent dynamic response of Guangxi marine soft foundation under traffic load(J). *Journal of Intelligent & Fuzzy Systems*, 2019, 37(4): 4811-4818.
- MA Lin, ZHANG Jun, LIU Yaming. Study on the Dynamic Characteristics of Remolded Loess in Shanxi Expressway Subgrade under Vehicle Loads(J). *China Earthquake Engineering Journal*, 2018, 40(01): 101-104.
- Meng Shangjiu, Zhou Jian, Wang Miao. Analysis on the deformation characteristics for roadbed under vehicle loads(J). *Earthquake Engineering and Engineering Dynamics*, 2018, 38(02): 35-41.
- O'connor A, O'Brien E J. Traffic load modelling and factors influencing the accuracy of predicted extremes(J). *Canadian Journal of Civil Engineering*, 2005, 32(1): 270-278.
- Qi H, Zhang X, Liu J, et al. Study on Deformation Characteristics of Low-Highway Subgrade under Traffic Load(J). *Applied Sciences*, 2022, 12(7): 3406.
- Shi Gang, Wang Yuyu, Wu Tianyi. Model Experiments on Ground Collapse under Traffic Roads(J). *Chinese Journal of Underground Space and Engineering*, 2020, 16(04): 1202-1209.
- Thevakumar K, Indraratna B, Ferreira F B, et al. The influence of cyclic loading on the response of soft subgrade soil in relation to heavy haul railways(J). *Transportation Geotechnics*, 2021, 29: 100571.
- Wang Rui, Wang Lei, Hu Zhiping. Steady States of Compacted Loess under Long term Traffic Loading(J). *Journal of Railway Engineering Society*, 2021, 38(01): 7-12.

- Wang Xinzhi, Chen Min, Wei Houzhen. Experimental study on dynamic response of calcareous sand subgrade under vehicle load(J). *Rock and Soil Mechanics*, 2018, 39(11): 4093-4101.
- Yang Qiangqiang, Ding Xiaojun, Wang Xu. Study on Vertical Earth Pressure Transfer Rule of Loess Subgrade under Vehicle Loading(J). *Journal of Highway and Transportation Research and Development*, 2021, 38(02): 40-47.
- Ye Bin, Ye Weimin, Feng Shouzhong. Dynamic Analysis of Silt Subgrade Under Traffic Loads(J). *Journal of Tongji University (Natural Science)*, 2012, 40(08): 1135-1141.
- Yu Huan, Zheng Junjie, Cao Wenzhao. Dynamic Characteristics Analysis of Widening Embankments under Asymmetric Traffic Loading(J). *China Earthquake Engineering Journal*, 2017, 39(06): 1111-1117.
- Zhang Jun, Shen Junmin, Gen Tian. Study of Working Depth in port Ground under Heavy Vehicle Load(J). *Chinese Journal of Rock Mechanics and Engineering*, 2014, 33(S1): 2942-2949.
- Zheng Guochen, Xu Hangli, Qi Ai. Field Measurement and Numerical Simulation on Environmental and Vibration Effects Induced by Metro and Ground Traffic(J). *China Environmental Science*, 2020, 40(09): 4146-4154.